Original paper

Pumilio2, but not Pumilio1, expression is significantly increased in high-grade and metastatic gastroenteropancreatic neuroendocrine neoplasms

Patryk Kraiński[1], Andrzej Kluk[1], Jan Gruszczynski[2,3], Kacper Trębacz[4], Ewa Dwojak[1], Maciej Dorota[1], Paweł Antoni Kołodziejski[5], Aldona Wiesława Wozniak[1]

[1]Department of Clinical Pathology and Immunology, Poznan University of Medical Sciences, Poznan, Poland
[2]Institute of Computing Science, Poznan University of Technology, Poznan, Poland
[3]Poznan University of Medical Sciences, Poznan, Poland
[4]Mathematics and Information Science, Warsaw University of Technology, Warsaw, Poland
[5]Department of Animal Physiology and Biochemistry, Poznan University of Life Sciences, Poznan, Poland

Pumilio proteins (PUM1 and PUM2) are evolutionarily conserved RNA-binding proteins that regulate gene expression at the post-transcriptional level and have been implicated in tumourigenesis in various cancers. However, their role in gastroenteropancreatic neuroendocrine neoplasms (GEP-NENs) has not been previously investigated. This study aimed to evaluate the expression of PUM1 and PUM2 in GEP-NENs and determine their association with tumour grade and metastatic status.

Transcriptomic data (GSE98894) were analyzed using GEO2R to assess differential gene expression in primary tumours, lymph node metastases, and distant metastases. Additionally, immunohistochemical analyses were performed on formalin-fixed paraffin-embedded samples, and protein expression was quantified using digital image analysis. Statistical comparisons were conducted across tumour sites and grades (G1–G3).

At the mRNA level, PUM2 was significantly upregulated in distant metastases compared with primary tumours ($\log_2 FC = 0.151$; adjusted $p = 0.024$), whereas PUM1 showed no significant difference. Protein-level analyses confirmed expression of both proteins in all samples; however, only PUM2 was significantly elevated in high-grade (G3) tumours compared to G1/G2.

These findings suggest that PUM2, but not PUM1, is associated with tumour progression in GEP-NENs, although a causal role remains to be established.

Key words: Pumilio, gastroenteropancreatic neuroendocrine neoplasms.

Introduction

Neuroendocrine neoplasms (NENs) are rare tumours that originate from cells of the diffuse neuroendocrine system [1]. Because neuroendocrine cells are distributed throughout various organs, NENs can also arise at multiple anatomical sites. The most common locations for these tumours are the gastrointestinal (GI) tract, including the pancreas, and the lungs, with the former accounting for approximately two-thirds of all NENs [1]. Tumours arising within the GI tract and pancreas are referred to as gastroenteropancreatic neuroendocrine neoplasms (GEP-NENs) [1]. Although GEP-NENs are consid-

ered rare, their incidence has been steadily increasing. Epidemiological studies have reported a fivefold increase in the United States between 1975 and 2015, a twofold increase in the Netherlands from 1990 to 2010, and a thirteenfold increase in Asia from 1996 to 2015 [1].

Gastroenteropancreatic neuroendocrine neoplasms are classified into neuroendocrine tumours (GEP-NETs) and poorly differentiated neuroendocrine carcinomas based on histological features and proliferative activity [2]. Gastroenteropancreatic neuroendocrine carcinomas are inherently high-grade tumours and are characterized by more aggressive behavior compared to GEP-NETs [1]. Gastroenteropancreatic neuroendocrine tumours, in contrast, are further graded as G1, G2, or G3 according to the World Health Organization 5th edition classification, using mitotic count and Ki-67 proliferation index; the higher of the two values determines the final grade [2]. Higher tumour grades are generally associated with more aggressive clinical behavior and decreased survival [1].

Despite this classification framework, tumour behavior and prognosis can vary significantly, even within the same grade. While G1 tumours are considered less aggressive, they are still malignant neoplasms that have the potential to metastasize. This clinical variability highlights the need for a deeper understanding of their underlying tumour biology.

Pumilio proteins (PUM1 and PUM2) were first described in *Drosophila melanogaster*, where they were shown to play a key role in posterior patterning during embryonic development [3]. Pumilio proteins were later identified as evolutionarily conserved RNA-binding proteins that act as important post-transcriptional regulators across diverse eukaryotic species [3]. In humans, two Pumilio proteins have been characterized – Pumilio 1 (PUM1) and Pumilio 2 (PUM2) – encoded by genes located on chromosomes 1 and 2, respectively [4]. Both proteins contain a 36-amino-acid PUF domain, organized into eight tandem repeats, with each repeat recognizing a single nucleotide within the consensus UGUAHAUW motif in the 3′ untranslated region of target mRNAs. This motif, known as the Pumilio-binding element, mediates their regulatory activity [4]. To date, no studies have specifically examined the expression or functional role of PUM1 and PUM2 in GEP-NENs.

Given the marked clinical heterogeneity of GEP-NENs that is not fully explained by histological grade and the importance of post-transcription regulation in controlling cellular phenotype, we therefore sought to investigate the expression patterns of PUM1 and PUM2 in GEP-NENs, with particular emphasis on their association with tumour grade and metastatic status, in order to clarify their potential role in tumour progression.

Material and methods

Differential gene expression analysis

Differential gene expression analysis was performed using the GEO2R tool available on the Gene Expression Omnibus website. We utilized the GSE98894 dataset [5], which comprises 212 samples of GEP-NETs. Of these, 130 were primary tumours originating in the pancreas (83 samples), small intestine (44 samples), and rectum (3 samples), while the remaining 82 samples were metastases – to the lymph nodes (12 samples), to the mesentery (1 sample) and to the liver (69 samples).

As described on the dataset's webpage, expression profiling was conducted for all 212 samples using high-throughput sequencing on the Illumina HiSeq 2500 platform.

We divided the samples first into three groups: primary tumours, lymph node metastases, and distant metastases; and then into two groups: primary tumours and metastases (combining both lymph node and distant metastases). Differential gene expression analysis was carried out for the following comparisons:

- primary tumours vs. lymph node metastases,
- primary tumours vs. distant metastases,
- lymph node metastases vs. distant metastases,
- primary tumours vs. all metastases (combined group).

Next, to account for biological heterogeneity related to primary tumour origin, additional analyses were performed with site-specific cohorts. The pancreatic cohort comprised 83 primary tumours and 30 liver metastases, whereas the small-intestinal cohort included 44 primary tumours, 8 lymph node metastases, and 28 liver metastases.

The following comparisons were then performed:

- pancreas: primary tumours vs. liver metastases;
- small intestine:
  - primary tumours vs. lymph node metastases,
  - primary tumours vs. liver metastases,
  - lymph node metastases vs. liver metastases.

The analysis was performed using the default GEO2R settings. Differential expression for *PUM1* and *PUM2* was summarized as log fold change and adjusted *p*-value, with multiple-testing correction performed using the Benjamini-Hochberg false discovery rate method, a significance threshold set at 0.05, and no minimum $\log_2$ fold change cut off applied.

Case selection for digital image analysis

Samples from patients with GEP-NENs were identified through search of the University Clinical Hospital database. In total, 52 patients were initially identified. Of these, 2 patients had no available histopathological material within the Department and were

therefore excluded from the study. The remaining patients had formalin-fixed, paraffin-embedded (FFPE) tissue blocks available for review.

Evaluation yielded 74 potential tissue samples, including primary tumours, lymph node metastases, and distant metastases. Each patient could have one or more samples from multiple anatomical sites. A patient was included in the study if at least one of their samples remained eligible for further analysis.

Samples derived from autopsy material were excluded as not explicitly eligible under the approval granted by institutional bioethics committee. Additional exclusions were applied when there was insufficient amount of neoplastic tissue within the paraffin block to permit further sectioning. Following regulations of the Polish Society of Pathology, and in accordance with the approval of the bioethics committee, tissue could not be sectioned if no neoplastic tissue would remain within the FFPE block after sectioning. Some samples were also lost at the technical stage. Due to financial limitations of the research grant, a sample could only be stained once; therefore any technical error resulted in loss of that sample for further digital image analysis.

In total, 60 samples from 43 patients were successfully analyzed, including 58 that were evaluated for PUM1 and 59 for PUM2. The difference in the number of cases of PUM1 and PUM2 was caused by the aforementioned loss at the technical stage. Taking all of this into account, the study represents a retrospective convenience cohort.

Immunohistochemistry

Formalin-fixed, paraffin-embedded tissue blocks were retrieved and sectioned into 4 μm-thick slices by the same person under the same conditions, which were then mounted on adhesive microscope slides (SuperFrost® Plus, Menzel Gläser). Immunohistochemical staining was performed using standard protocols. Heat-induced epitope retrieval was carried out at 97°C in a water bath for 40 minutes using the EnVision FLEX Target Retrieval Solution (high pH). This was followed by automated immunohistochemical staining on the Autostainer Link 48 system (Agilent/Dako), employing the EnVision FLEX+ System (High pH) visualization kit. For detection of PUM proteins, Invitrogen polyclonal antibodies against PUM1 (PA530327) and PUM2 (PA528705) were used at a dilution of 1:150, with an incubation time of 1 hour. Testis tissue served as the positive control for both PUM1 and PUM2.

Digital image analysis of Pumilio1 and Pumilio2 protein expression

The stained slides were scanned at 20× objective using the Ventana DP 200 scanner, and images were saved in TIFF format. Digital image analysis was performed using quantified digital image analysis (QuPath) software. Tumour regions were manually annotated by a board-certified pathologist (PK). Normal tissue was not analyzed within this study. Cell detection was conducted using QuPath's builtin cell detection tool, with default settings except for the intensity threshold. Intensity threshold was empirically optimized (set to 0.04) by PK to achieve most accurate cell detection based on visual inspection of segmentation results. A random forest classifier was then applied within QuPath to categorize cells into tumour and non-tumour populations. For subsequent quantitative analysis, 3,3'-diaminobenzidine optical density (DAB OD mean) was used as the measure of protein expression. Quantification was performed separately for the nucleus cytoplasm, and whole cell compartments. The expression levels of PUM1 and PUM2 were analyzed across primary tumours (T), lymph node metastases (N), and distant metastases (M) and across different histological grades (G1, G2, G3).

To further assess expression levels, values were aggregated at the sample level using Python's Pandas library, and categorized into the following expression groups:

- negative (< 0.1),
- very weak (≥ 0.1 and < 0.2),
- weak (≥ 0.2 and < 0.4),
- moderate (≥ 0.4 and < 0.6),
- strong (0.6).

These cut-offs were based on QuPath's default thresholds, with the exception of the "very weak" category, which was introduced to better capture low-level expression observed in some samples previously labeled as negative.

Statistical analysis

To assess whether there are statistically significant differences in levels of Nucleus DAB OD mean, Cell DAB OD mean, or Cytoplasm DAB OD mean in cells from different slide types or tumour grades, a linear mixed-effects model was used. The use of linear mixed-effects model was motivated by heterogenous and partially paired structure of the dataset, in which samples originated from different patients, while individual patients could contribute one, two or three samples from different anatomical sites. Consequently, observations were neither fully independent nor fully paired, making standard statistical approaches inappropriate and potentially misleading.

Measurements with values lower than the background level (0) were deleted. Then, due to the long-tailed distribution of the data, values were log-transformed. To reduce computational load while maintaining representative data, up to 100,000 sample measurements were randomly selected from each image.

Linear mixed-effects model was then fitted for each measured value. Three models were fitted for each pair of slide types, and one model was fitted to compare

tumour (T) vs. combined metastases (NM). The same analysis was performed for tumour grading, with models fitted for each pairwise comparison, followed by one model comparing G1 + G2 vs. G3 tumours. Adjusted *p*-value was calculated with multiple-testing correction performed using the Benjamini-Hochberg false discovery rate method. A significance threshold was set at 0.05.

Software (including AI) use

Quantified using digital image analysis was utilized for digital image analysis, including image annotation, quantification, and extraction of relevant features. Most data analyses and visualizations were conducted using Python. The Pandas library was used for data manipulation, while Seaborn and Matplotlib were employed to generate figures and visualize results. R was used for specific statistical modeling, particularly for linear mixed-effects models. These were fitted using the lme4 package, with *p*-values for fixed effects calculated using the lmerTest package. Zotero was used for reference and citation management throughout the research and writing process. ChatGPT (OpenAI) was used to support editing of this manuscript, providing assistance with language refinement, clarity enhancement, and adaptation of tone.

Results

Pumilio2, but not Pumilio1, is significantly upregulated in metastatic pancreatic neuroendocrine tumours

In the global comparisons separating primary tumours, lymph-node metastases, and distant metastases, *PUM1* expression did not differ significantly between groups. Adjusted *p*-values ranged 0.077–0.499.

Similar findings were observed for PUM1 in site-specific analyses. In pancreatic tumours, comparison of primary lesions and liver metastases showed a non-significant increase in metastases ($\log_2$ fold change = 0.185; adjusted $p = 0.13$). In small-intestinal tumours, none of the comparisons reached statistical significance, including primary vs. lymph node meta-stases, primary vs. liver metastases, and lymph node vs. liver metastases.

In contrast, *PUM2* expression demonstrated modest but statistically significant increases in metastatic samples in the global analysis. Expression was higher in distant metastases compared with primary tumours ($\log_2$ fold change = 0.151; adjusted $p = 0.024$) and in metastases analyzed as a combined group relative to primary tumours ($\log_2$ fold change = 0.141; adjusted $p = 0.025$). These correspond to approximately 11% and 10% increases in expression, respectively. The remaining comparisons did not yield statistically significant results.

When analyses were restricted to biologically-matched cohorts, statistical significance persisted only in pancreatic neuroendocrine tumours, where liver metastases exhibited higher *PUM2* expression than primary tumours ($\log_2$ fold change = 0.220; adjusted $p = 0.042$). No statistically significant differences were observed in small-intestinal tumours, including comparisons of primary tumours with lymph node metastases, primary tumours with liver metastases or lymph node with liver metastases.

Overall, these findings indicate that metastasis-associated upregulation of *PUM2* is modest and appears to be driven primarily by pancreatic tumours, whereas *PUM1* shows no significant differential expression in gastroenteropancreatic neuroendocrine neoplasms.

Pumilio proteins are expressed in gastroenteropancreatic neuroendocrine neoplasms

A total of 43 patients with GEP-NENs were included in the final analysis, yielding 60 successfully analyzed tissue samples. Among the patients, 27 were male and 16 were female. Of the 60 analyzed samples, 38 were classified as G1, 12 as G2, and 10 as G3. Thirty-four samples represented primary tumours. The large intestine was the most common primary site ($n = 12$), followed by the small intestine ($n = 9$), stomach ($n = 6$), pancreas ($n = 3$), appendix ($n = 2$), esophagus ($n = 1$), and retroperitoneum ($n = 1$). In addition, there were 8 lymph node metastases and 18 distant metastases. The most frequent metastatic site was the liver ($n = 9$), followed by the mesentery ($n = 5$), nasal cavity ($n = 2$), and the omentum ($n = 2$).

Cytoplasmic DAB OD mean values for PUM1 ranged 0.101–0.540, with a mean of 0.248. For PUM2, values ranged 0.115–0.651, with a mean of 0.293. The kernel density estimation plots illustrating the distribution of cytoplasmic DAB OD mean values for both proteins are presented in Figure 1.

Using these categories:

- PUM1 cytoplasmic expression was observed in all 58 samples: 22 out of 58 were classified as very weak, 29 as weak, and 7 as moderate. No samples showed strong expression;
- PUM2 cytoplasmic expression was also present in all 59 samples: 12 were very weak, 38 weak, 8 moderate, and 1 sample exhibited strong expression.

Representative immunohistochemical images illustrating PUM1 and PUM2 expression categories in GEP-NENs are shown in Figures 2–8.

Expression of Pumilio proteins does not change significantly across different sites

Analysis of PUM1 expression revealed that in primary tumours, PUM1 expression levels were lowest, with mean DAB OD values of 0.171 in the cytoplasm

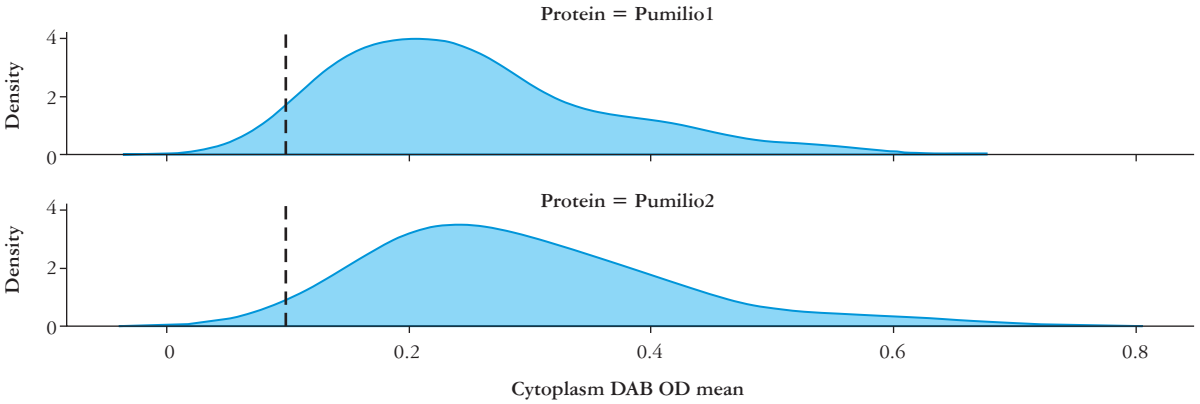

Figure 1. The kernel density estimation plots illustrating the distribution of cytoplasmic 3,3'-diaminobenzidine optical density mean values for both proteins

DAB OD – 3,3'-diaminobenzidine optical density

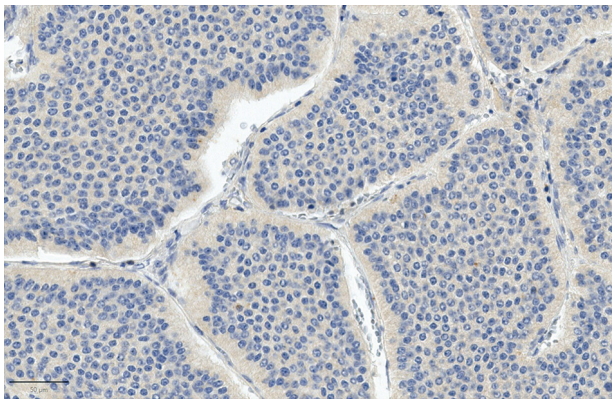

Figure 2. Representative immunohistochemical staining for Pumilio1 demonstrating the very weak cytoplasmic expression category in a metastatic gastroenteropancreatic neuroendocrine tumour

The image was obtained from tumour tissue within a liver metastasis, with no surrounding hepatic parenchyma visible in the field of view (200×).

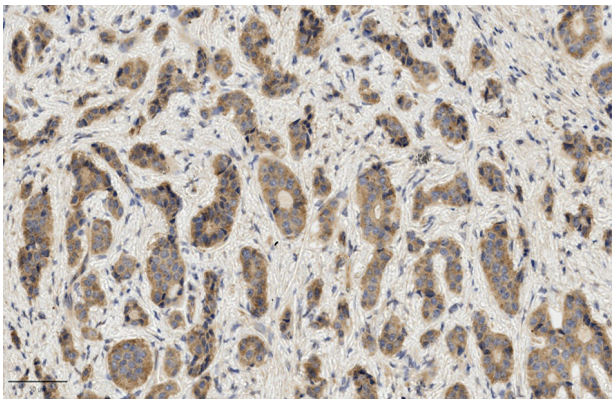

Figure 3. Representative immunohistochemical staining for Pumilio1 demonstrating the weak cytoplasmic expression category in a metastatic gastroenteropancreatic neuroendocrine tumour

The image was obtained from tumour tissue within a mesenteric metastasis, and only tumour tissue is present in the field of view (200×).

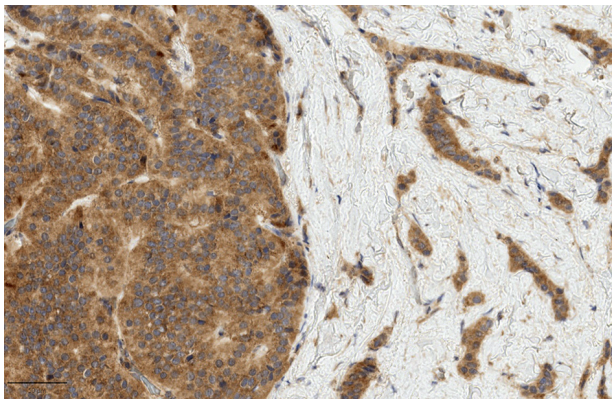

Figure 4. Representative immunohistochemical staining for Pumilio1 demonstrating the moderate cytoplasmic expression category in a gastroenteropancreatic neuroendocrine tumour

The image was obtained from tumour tissue located in the submucosa of the rectum, and only neoplastic cells within the submucosal compartment are visible in the field of view (200×).

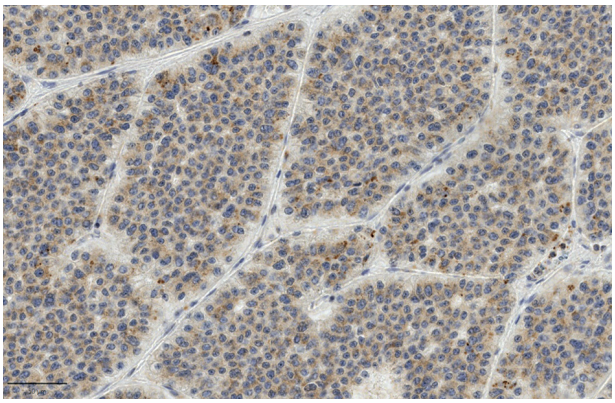

Figure 5. Representative immunohistochemical staining for Pumilio2 demonstrating the very weak cytoplasmic expression category in a metastatic gastroenteropancreatic neuroendocrine tumour

The image was obtained from tumour tissue within a mesenteric metastasis, and only tumour cells are visible in the field of view (200×).

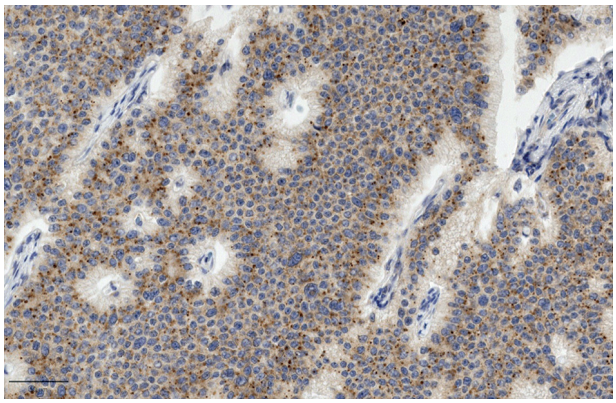

Figure 6. Representative immunohistochemical staining for Pumilio2 demonstrating the weak cytoplasmic expression category in a metastatic gastroenteropancreatic neuroendocrine tumour

The image was obtained from tumour tissue within a mesenteric metastasis, and only tumour cells are visible in the field of view (200×).

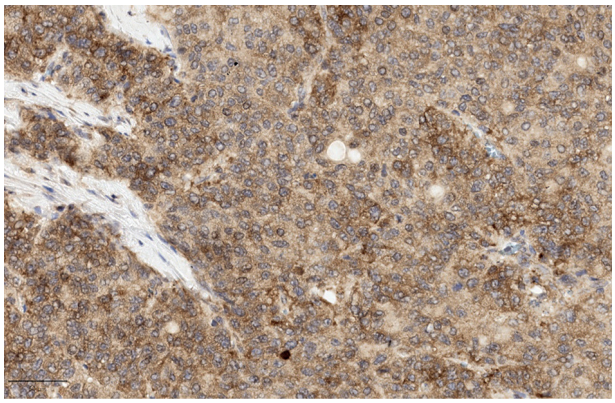

Figure 7. Representative immunohistochemical staining for Pumilio2 demonstrating the moderate cytoplasmic expression category in a metastatic gastroenteropancreatic neuroendocrine tumour

The image was obtained from tumour tissue within an omental metastasis, and only tumour cells are visible in the field of view (200×).

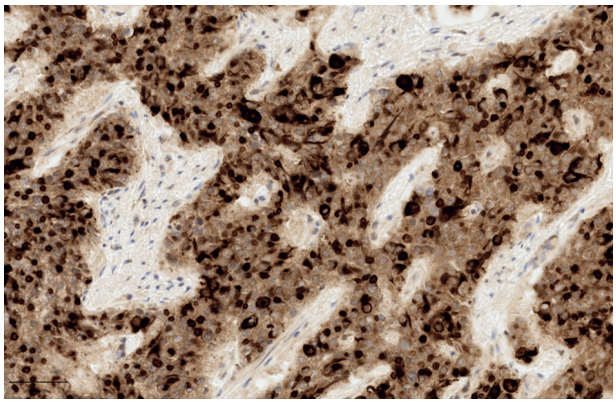

Figure 8. Representative immunohistochemical staining for Pumilio2 demonstrating the strong cytoplasmic expression category in a gastroenteropancreatic neuroendocrine tumour

It also demonstrates strong perinuclear and possibly nuclear expression. The image was obtained from tumour tissue located in the submucosa of the small intestine, and only tumour cells are visible in the field of view (200×).

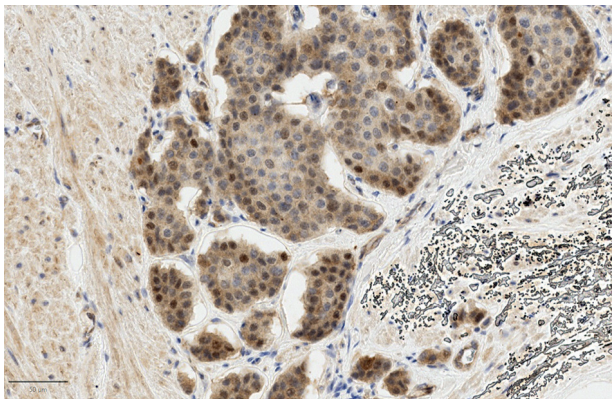

Figure 9. Representative immunohistochemical staining for Pumilio1 demonstrating cytoplasmic and some possible nuclear expression in a gastroenteropancreatic neuroendocrine tumour

The image was obtained from tumour tissue located in the muscular wall of the small intestine, and only tumour cells and smooth muscle are visible in the field of view (200×).

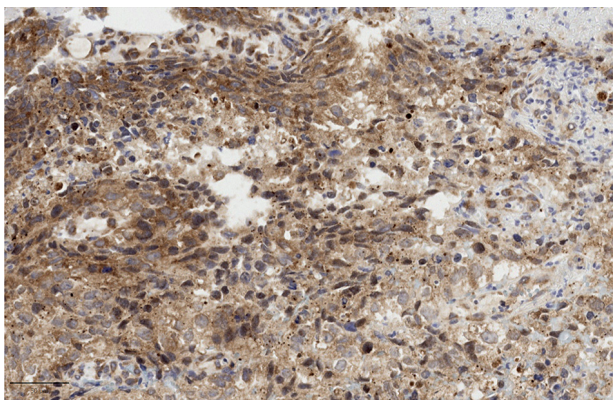

Figure 10. Representative immunohistochemical staining for Pumilio2 demonstrating cytoplasmic and some possible nuclear expression in a gastroenteropancreatic neuroendocrine tumour

The image was obtained from tumour tissue located in the wall of the esophagus, and only tumour cells are visible in the field of view (200×).

and 0.169 at the whole cell level. Expression increased markedly in lymph node metastases, reaching mean values of 0.283 (cytoplasmic), and 0.288 (whole cell). In distant metastases (M), levels decreased but still remained higher compared to primary tumours, with means of 0.212 (cytoplasmic) and 0.216 (whole cell).

Pumilio2 showed a similar pattern. In primary tumours, mean OD values were 0.268 in the cytoplasm and 0.267 across the whole cell. Expression was highest in lymph node metastases, with means of 0.325 (cytoplasm) and 0.325 (whole cell). A subsequent decrease was observed in distant metastases, where values dropped to 0.265 (cytoplasm), and 0.253 (whole cell).

PUM2 expression is increased in high-grade tumours

Expression of PUM1 remained relatively stable across different tumour grades. Cytoplasmic DAB OD

mean values slightly decreased from grade 1 (0.219) to grade 2 (0.171), followed by an increase in grade 3 (0.270). A similar trend was observed in whole cell DAB OD mean values (G1: 0.214; G2: 0.172; G3: 0.271). Despite the apparent rise in grade 3, statistical analysis did not show any significant differences in PUM1 expression between different grades.

In contrast, PUM2 showed an increase in expression in higher-grade tumours. Cytoplasmic DAB OD mean values remained relatively unchanged between G1 (0.250) and G2 (0.247), but increased substantially in G3 (0.402). Whole cell measurements followed the same pattern (G1: 0.253; G2: 0.253; G3: 0.409).

When comparing combined low-grade tumours (G1 and G2) to high-grade tumours (G3), statistically significant increases in PUM2 expression were observed in both compartments: cytoplasm ($p = 0.007$), and whole cell ($p = 0.007$). A similar change was observed for comparison of G1 with G3: cytoplasm ($p = 0.007$), and whole cell ($p = 0.007$). No significant differences were identified in other pairwise comparisons between individual grades.

These results indicate that PUM2 expression is specifically increased in high-grade tumours, while PUM1 remains largely unaffected by the tumour grade.

Possible nuclear expression of Pumilio1 and Pumilio2

Using QuPath, the nuclear DAB OD mean was also assessed within an automatically derived nuclear compartment. For PUM1, the mean values ranged 0.120–0.597, with a mean of 0.243. When stratified by disease site, the lowest mean nuclear signal was observed in primary tumours (0.180), while higher values were detected in lymph node metastases (0.276). In distant metastases, the mean nuclear value decreased to 0.209 but remained higher than in primary tumours.

For PUM2, nuclear DAB OD mean values ranged 0.130–1.073, with a mean of 0.321. The mean nuclear signal was 0.275 in primary tumours and increased to 0.331 in lymph node metastases. In distant metastases, the value decreased to 0.296.

No case demonstrated exclusively nuclear staining in the absence of cytoplasmic expression. In several samples, low levels of signal were detected within the nuclear compartment by automated analysis despite the predominance of cytoplasmic staining on visual inspection (Figures 1–7). In such instances, automated nuclear segmentation may have captured a small portion of cytoplasm immediately surrounding the nucleus. Consequently, a fraction of the signal quantified within the nuclear compartment may actually reflect cytoplasmic staining adjacent to the nuclear membrane rather than true nuclear localization.

In some tumours, more pronounced perinuclear accumulation of staining was observed, which in two-dimensional histological sections may be difficult to distinguish from true nuclear localization and was captured as a nuclear signal by QuPath (Figure 8).

At the same time, in some of the samples, focal staining within the nuclear interior was observed (Figures 9 and 10). Therefore, although part of the quantified signal may represent perinuclear or juxtanuclear cytoplasmic staining captured by automated segmentation, true nuclear expression cannot be completely excluded. For completeness, nuclear compartment measurements are therefore reported, and representative images illustrating apparent nuclear signal of PUM1 and PUM2 are shown in Figures 8–10.

Discussion

The role of RNA-binding proteins in the pathogenesis of GEP-NENs remains largely unexplored. Among these, PUM1 and PUM2 are best known for their evolutionary conservation and roles in embryonic development, stem cell maintenance, and post-transcriptional regulation [3]. Increasingly, however, it has also been shown they may play a role in tumourigenesis across a range of neoplasms [6]. To our knowledge, this is the first study to systematically assess PUM1 and PUM2 expression in GEP-NENs at both the transcriptomic and protein levels.

Our integrated analysis provides two key insights. First, we demonstrate that both PUM1 and PUM2 are expressed in GEP-NENs which is a novel finding, as their presence in these tumours has not previously been documented. Second, their biological roles appear to diverge. While PUM1 expression remained relatively stable across tumour grades and metastatic sites, PUM2 was significantly upregulated in high-grade tumours at the protein level. A less pronounced, but a significant increase was also observed in metastatic lesions in pancreatic neuroendocrine tumours at the mRNA level. This pattern suggests that PUM1 may serve a more constitutive "housekeeping" role, whereas PUM2 may have some association with aggressive tumour behavior in pancreatic neuroendocrine tumours.

The differential involvement of PUM1 and PUM2 in cancer aligns with prior reports across malignancies. PUM1 has been shown to be overexpressed in pancreatic, gastric, and ovarian cancers compared with normal tissues, and its expression is associated with proliferation, migration, and invasion in pancreatic and ovarian cancers [7–9]. In colon cancer, both mRNA and protein levels of PUM1 are elevated in metastases compared with normal tissue, and silencing reduces metastatic burden [10]. Similarly, in gastric cancer, PUM1 knockdown decreased peritoneal metastasis *in vivo* [9]. Pumilio2 has been implicated as a poor prognostic factor in hepatocellular carcino-

ma and breast cancer, while in glioblastoma, its inhibition suppresses proliferation and invasion [11–13]. Yet its role is not uniformly oncogenic – osteosarcoma represents a counterexample, where PUM2 is downregulated and exerts tumour-suppressive effects [14]. Collectively, these findings show that PUM1 and PUM2 act in a highly context-dependent manner, with tumour-type-specific functions.

Both PUM1 and PUM2 are RNA-binding proteins predominantly located in the cytoplasm, where they exert most of their activity. Immunofluorescence studies of PUM1 showed that it is expressed in the cytoplasm of spermatocytes and other germ cells, which was further confirmed by immunoblot analysis of cytoplasmic and nuclear fractions [15]. According to the authors, this is consistent with findings in other species such as *Drosophila* and *C. elegans* [15]. In the brain, PUM2 has been reported to be expressed in the cell body and dendrites [16].

Interestingly, in our study, we found some expression of both PUM1 and PUM2 in the nucleus of neoplastic cells. However, considering the literature on the subcellular localization of PUM1 and PUM2, these findings appear unexpected and warrant careful interpretation.

One possibility is that PUM1 and PUM2 may, under certain conditions, enter the nucleus and perform specific functions, although this has not been directly demonstrated as for other proteins [17]. Another explanation is that proteolysis or alternative splicing may generate shorter PUM fragments capable of translocating to the nucleus, where their epitopes are then detected.

Importantly, nuclear localization of PUM1 and PUM2 has already been reported in some studies. Moore *et al*. [18] showed that the DAZL:PUM2 protein can be found both in the cytoplasm and the nucleus of spermatogonia, which provides evidence that nuclear presence of PUM2 might be possible under certain conditions. In addition, publicly available immunofluorescence data from the Human Protein Atlas indicate that, while PUM1 and PUM2 are predominantly cytoplasmic in most analyzed human cell lines, partial nucleoplasmic or nuclear-adjacent localization can be observed in selected models (e.g. A-431, U-251MG, U2OS) [19]. Although these are isolated reports, and the majority of the research points toward cytoplasmic localization of those proteins, they nonetheless suggest that the nuclear signal is not entirely absent in certain contexts.

More likely in our case, these findings reflect technical limitations of digital image analysis and its ability to resolve subcellular localization. Automatic segmentation of QuPath also includes, to some extent, the perinuclear region and may therefore inadvertently capture cytoplasmic signal as nuclear signal. This appears most plausible explanation, particularly when the quantitative values are interpreted alongside the images. In Figures 1–7 some degree of expression was detected by QuPath, although careful inspection suggests that this signal most likely originates from the nuclear border and is actually cytoplasmatic. Some cases may also show pronounced perinuclear accumulation that is difficult to distinguish from true nuclear staining in two-dimensional imaging, as illustrated in Figure 8.

Nevertheless, there are cases in which nuclear signal cannot be excluded, as shown in Figures 9 and 10. However, even if this represents true nuclear expression, it should be interpreted with caution. Possible explanations include cross-reactivity with a structurally related nuclear protein, poor tissue fixation leading to artifactual leakage of proteins into the nucleus [20, 21]. Furthermore, it cannot be excluded that the antibodies used recognize truncated PUM protein isoforms or proteolytic fragments with altered intracellular localization.

Overall, the nuclear localization of PUM1 and PUM2 observed in our study should be regarded rather as a hypothesis-generating finding than definitive evidence of a novel nuclear function. We cannot completely exclude that this observation reflects a technical artifact rather than true staining. However, we believe that this observation merits reporting, as it may serve as a starting point for further investigations. Nevertheless, independent validation using additional approaches – such as different antibodies, immunofluorescence, or biochemical fractionation – is required to confirm or refute true nuclear localization in neuroendocrine neoplasms.

Taken together, our results suggest that PUM2, but not PUM1, is associated with higher tumour grade in GEP-NENs at the protein level, with additional evidence of increased expression in metastatic samples in pancreatic neuroendocrine tumours at the mRNA level. While these findings may suggest a possible link between PUM2 expression and more advanced disease, they do not establish a causal role in tumour aggressiveness. Further studies are needed to clarify the biological and clinical significance of PUM1 and PUM2 in GEP-NENs.

Limitations of the study

Several limitations of the present study should be acknowledged.

First, the transcriptomic analysis was based on a publicly available dataset (GSE98894), which, although relatively large, contains tumours originating from different anatomical sites. While additional site-specific analyses were performed to partially address this heterogeneity, the dataset does not include complete clinical annotations, including histological grading information. As a result, transcriptomic

comparisons according to tumour grade could not be performed. Furthermore, the observed differences in PUM2 expression at the mRNA level were relatively modest and appeared to be driven primarily by pancreatic neuroendocrine tumours, which limits the generalizability of these findings across all gastroenteropancreatic neuroendocrine neoplasms.

Second, the immunohistochemical cohort represents a retrospective single-center series with a relatively limited number of cases. In addition, individual patients contributed samples from different anatomical sites, while other patients were represented by only a single specimen, resulting in a heterogeneous dataset with partially paired observations. The number of cases within specific anatomical and subgroups was also limited, which prevented detailed subgroup analyses according to tumour origin.

Third, the small number of G3 tumours in the immunohistochemical cohort ($n = 10$) limits the statistical power of grade-based comparisons. Although statistically significant differences were observed between G3 and lower-grade tumours, these findings should be interpreted cautiously and considered exploratory until validated in larger, independent cohorts with more adequate high-grade tumour representation.

Fourth, the quantitative assessment of protein expression was based on digital image analysis and optical density measurements. Although this approach provides an objective and reproducible method for quantifying immunohistochemical staining, optical density may still be influenced by technical factors such as staining variability, section thickness, and tissue processing. To minimize such variability, all samples were processed under standardized conditions by the same person, using the same automated staining platform and digital analysis pipeline. Nevertheless, optical density measurements should be interpreted primarily as a research tool rather than a direct diagnostic or clinical metric.

Another limitation concerns the interpretation of the nuclear signal detected for PUM1 and PUM2 which should be interpreted with caution for reasons presented in the results and discussion sections.

Conclusions

The present study is observational in nature and demonstrates associations between PUM2 expression, tumour grade, and metastatic status rather than establishing a causal relationship. Functional studies will be required to clarify the biological role of PUM1 and PUM2 in GEP-NENs and to determine whether PUM2 contributes directly to tumour progression.

Disclosures

1. Institutional review board statement: The study was conducted in accordance with the Declaration of Helsinki and the regulations outlined in the standards and guidelines of the Polish Society of Pathology.
2. Assistance with the article: None.
3. Financial support and sponsorship: The project was funded by the National Science Centre, Poland, grant number 2021/41/N/NZ7/03146.
4. Conflicts of interest: None.

References

1. Zhang X Bin, Fan YB, Jing R, Getu MA, Chen WY, Zhang W, et al. Gastroenteropancreatic neuroendocrine neoplasms: current development, challenges, and clinical perspectives. Mil Med Res 2024; 11: 35.
2. Klimstra DS, Günter K, La Rosa S, Rindi G. Classification of neuroendocrine neoplasms of the digestive system. WHO Classification of tumours, 5 edition, 2019.
3. Nishanth MJ, Simon B. Functions, mechanisms and regulation of Pumilio/Puf family RNA binding proteins: a comprehensive review. Mol Biol Rep 2020; 47: 785-807.
4. Smialek MJ, Ilaslan E, Sajek MP, Jaruzelska J. Role of PUM RNA-binding proteins in cancer. Cancers (Basel) 2021; 13: 129.
5. Alvarez MJ, Subramaniam PS, Tang LH, Grunn A, Aburi M, Rieckhof G, et al. A precision oncology approach to the pharmacological targeting of mechanistic dependencies in neuroendocrine tumors. Nat Genet 2018; 50: 979-989.
6. Silva ILZ, Kohata AA, Shigunov P. Modulation and function of Pumilio proteins in cancer. Semin Cancer Biol 2022; 86: 298-309.
7. Dai H, Jiang Y, Liu Z, Su X, Yang Y, Chen Z. Pumilio RNA-binding family member 1 plays a promoting role on pancreatic cancer angiogenesis. Can J Gastroenterol Hepatol 2022; 2022: 9202531.
8. Guan X, Chen S, Liu Y, Wang L li, Zhao Y, Zong ZH. PUM1 promotes ovarian cancer proliferation, migration and invasion. Biochem Biophys Res Commun 2018; 497: 313-318.
9. Yin S, Liu H, Zhou Z, Xu X, Wang P, Chen W, et al. PUM1 promotes tumor progression by activating DEPTOR-meditated glycolysis in gastric cancer. Adv Sci 2023; 10: e2301190.
10. Gor R, Sampath SS, Lazer LM, Ramalingam S. RNA binding protein PUM1 promotes colon cancer cell proliferation and migration. Int J Biol Macromol 2021; 174: 549-561.
11. Liu Z, Lv C. RNA binding protein PUM2 promotes hepatocellular carcinoma proliferation and apoptosis via binding to the 3'UTR of BTG3. Oncol Lett 2022; 24: 346.
12. Wang Y, Sun W, Yang J, Yang L, Li C, Liu H, et al. PUM2 promotes glioblastoma cell proliferation and migration via repressing BTG1 expression. Cell Struct Funct 2019; 44: 29-39.
13. Zhang L, Chen Y, Li C, Liu J, Ren H, Li L, et al. RNA binding protein PUM2 promotes the stemness of breast cancer cells via competitively binding to neuropilin-1 (NRP-1) mRNA with miR-376a. Biomed Pharmacother 2019; 114: 108772.
14. Hu R, Zhu X, Chen C, Xu R, Li Y, Xu W. RNA-binding protein PUM2 suppresses osteosarcoma progression via partly and competitively binding to STARD13 3′UTR with miRNAs. Cell Prolif 2018; 51: e12508.
15. Chen D, Zheng W, Lin A, Uyhazi K, Zhao H, Lin H. Pumilio 1 suppresses multiple activators of p53 to safeguard spermatogenesis. Curr Biol 2012; 22: 420-425.
16. Vessey JP, Vaccani A, Xie Y, Dahm R, Karra D, Kiebler MA, et al. Dendritic localization of the translational repressor Pumilio 2 and its contribution to dendritic stress granules. J Neurosci 2006; 26: 6496-6508.
17. Gilbertson S, Federspiel JD, Hartenian E, Cristea IM, Glaunsinger B. Changes in mRNA abundance drive shuttling

of RNA binding proteins, linking cytoplasmic RNA degradation to transcription. Elife 2018; 7: e37663.
18. Moore FL, Jaruzelska J, Fox MS, Urano J, Firpo MT, Turek PJ, et al. Human Pumilio-2 is expressed in embryonic stem cells and germ cells and interacts with DAZ (Deleted in AZoospermia) and DAZ-like proteins. Proc Natl Acad Sci U S A 2003; 100: 538-543.
19. Uhlén M, Fagerberg L, Hallström BM, Lindskog C, Oksvold P, Mardinoglu A, et al. Tissue-based map of the human proteome. Science 2015; 347: 1260419.
20. Melan MA, Sluder G. Redistribution and differential extraction of soluble proteins in permeabilized cultured cells: implications for immunofluorescence microscopy. J Cell Sci 1992; 101: 731-743.
21. Shi SR, Shi Y, Taylor CR. Antigen retrieval immunohistochemistry. J Histochem Cytochem 2011; 59: 13-32.

Address for correspondence

Paweł Antoni Kołodziejski
Department of Animal Physiology and Biochemistry
Poznan University of Life Sciences
Poznan, Poland
e-mail: pawelbigi@gmail.com, pawel.kolodziejski@up.poznan.pl